

Isotope evidence for quantifying river evaporation and recharge processes in the lower reaches of the Yellow River

Xin Zhao^{1,2} · Fadong Li^{1,2}

Received: 26 February 2016 / Accepted: 24 January 2017 / Published online: 3 February 2017
© Springer-Verlag Berlin Heidelberg 2017

Abstract Evaporation and recharge are important hydrological processes in the water cycle. However, accurately quantifying these two processes of river remains to be difficult due to their spatial heterogeneity and the limitations of traditional methods. In this study, a more reliable method of stable isotopes of $\delta^{18}\text{O}$ and $\delta^2\text{H}$ based on the Rayleigh distillation equation and mass conservation was used to estimate the evaporation and recharge of the rivers in the lower reaches of the Yellow River, North China Plain. Comprehensive sampling campaigns including 30 surface water samples from 10 rivers, 33 groundwater samples from domestic and observation wells, and two Yellow River water samples were conducted. The results showed that the evaporation proportion of the rivers based on $\delta^{18}\text{O}$ and $\delta^2\text{H}$ both averaged 14.4%. The evaporation proportions in each river did not completely follow a linear increasing trend along the flow path. This phenomenon could be mainly explained by the different proportions of recharge from groundwater and Yellow River water. With closer to the Yellow river, evaporation of the rivers decreased while the recharge by the Yellow River increased. Regression equations based on $\delta^{18}\text{O}$, $\delta^2\text{H}$, and their average revealed that the evaporation proportion respectively increased by 1.02, 0.79, and 0.90% with the increase in the distance to the Yellow River per 10 km. On

the contrary, the recharge proportion decreased by 7.68, 5.51, and 6.59%, respectively. In addition, using $\delta^{18}\text{O}$ rather than $\delta^2\text{H}$ was more reliable in studying the spatial influence of the Yellow River on evaporation and recharge. Sensitivity analysis showed that the evaporation model was most sensitive to isotopic composition, rather than to air temperature or relative humidity. The results of this study provide insights into the determination of river hydrological processes and the management of water resources.

Keywords Flow path · Groundwater · Hydrological process · Rayleigh distillation · Stable isotope · Yellow River

Introduction

Understanding the variations in isotopic compositions of water contributes to trace the process of hydrological cycle, especially for evaporation and recharge (Yakir and Sternberg 2000). Former studies related to the evaporation (Brooks et al. 2014; Gibson and Edwards 2002; Gibson et al. 1993; Qian et al. 2014; Wang et al. 2014) and recharge (Krabbenhoft et al. 1990; Steinbruch and Weise 2014; Wood and Sanford 1995) have focused on lakes, and little attention has been paid to rivers (Daniel 2015; Maheu et al. 2014). It is relatively easy to determine a lake's evaporation for a known inflow and outflow, slow circulation, and high stability (Skrzypek et al. 2015). However, an evaporation estimation of rivers at the catchment scale is difficult due to the complex interaction of surface water and groundwater along the flow path caused by surface water diversion, river flows alteration, and reservoir or dam construction (Xu and Singh 1998). Changes in the isotopic composition of water may be altered by environmental

✉ Fadong Li
lifadong@igsnr.ac.cn

¹ Key Laboratory of Ecosystem Network Observation and Modeling, Institute of Geographic Sciences and Natural Resources Research, Chinese Academy of Sciences, 11A, Datun Road, Chaoyang District, Beijing 100101, China

² College of Resources and Environment, University of Chinese Academy of Sciences, Beijing 100190, China

factors derived by physically and biologically mitigated processes (Paces and Wurster 2014). The unique climatology and hydrology characteristics of each individual river make different rivers follow different evaporation patterns (Jasechko et al. 2013). In addition, different sites along the flow path at each river exhibit their own unique temperature, relative humidity, wind speed, and fetch, which results in different evaporation proportions (Gibson et al. 1993). Meanwhile, isotopic compositions differ greatly at different sites due to the complex geological condition. Thus, identifying the source and relative contributions of multiple recharge at the catchment scale is not easy as well (Palmer et al. 2007). Overall, an accurate estimation of evaporation and recharge is crucial for better understanding the hydrological processes of rivers.

Traditional methods used to measure water evaporation are based on humidity change in the air stream, weight change of the water pan, water level change, and heat and mass balances (Ershadi et al. 2014; Hostetler and Bartlein 1990; Singh and Xu 1997; Xu et al. 2006). The stable isotopes of $\delta^{18}\text{O}$ and $\delta^2\text{H}$ is a valid new technique of ecological research and has been widely employed for tracing the origin, pathway, and behavior of water (Paces and Wurster 2014). The movement of water is the main driving force for biogeochemical cycles and water cycles (Richey et al. 1990), which consequently alters the isotopic composition of river water. Residual water is significantly depleted in $\delta^{18}\text{O}$ and $\delta^2\text{H}$ in comparison with the original water because the lighter isotopes are kinetically favored in the evaporation (Elmi et al. 2013). The loss of water might be recharged by groundwater or other rivers. Traditional estimations of recharge are based on measurements using piezometers, gravimeters, and seepage meters (Krabbenhoft et al. 1990; McCallum et al. 2014). These methods usually have difficulties in dealing with the spatial and temporal variability of meteorological and hydrological parameters throughout the year at the catchment scale (Gibson et al. 1993). Instead, using the method of stable isotopes to calculate river evaporation and recharge has apparent advantage of easily direct gauged that traditional method cannot match. Therefore, measurement of stable isotopes in rivers could provide direct recognizable evidence for the magnitude of integrated evaporation and recharge.

The North China Plain (NCP), the largest alluvial plain in China, is currently subject to increasingly severe water resources scarcity (Shen et al. 2013; Li et al. 2011; Liu et al. 2016). With the development of industrialization and urbanization, anthropogenic activities become increasingly prominent and lead to a series of hazardous influences related to this issue: such as decline of the groundwater levels, drying up of the rivers, and reducing the runoff (Wang et al. 2014). Irrigation as a common agricultural

practice accounts for the largest amount of water use in the NCP (Zhang et al. 2011). It is estimated that irrigation consumes up to 70 to 80% of the total water resource allocation (Chen et al. 2003). To alleviate this industrial, municipal, and agricultural water shortage, diverting water from a large river is an effective solution. As the second longest river in China, the Yellow River feeds about 107 million people in NCP (Wang et al. 2012). Hence, projects that divert water from the Yellow River have been implemented for more than 50 years (Qian et al. 2007). However, large-scale water diversion practices may disturb local hydrologic cycles and consequently alter the isotopic composition of the water. Thereafter the river's isotopic feature is unknown. Also, in the context of this large-scale water diversion project, the magnitude of the spatial influence of the Yellow River on evaporation and recharge is not clear.

To date, comprehensive data sets on evaporation and recharge deduced from stable isotopes are scarce in this area. Accordingly, in this study, a data set of samples from surface water and groundwater collected at several sites in the lower reaches of the Yellow River was analyzed using stable isotopes to determine the evaporation and recharge proportion of the rivers. The specific objectives of this study are: (1) to investigate the stable isotopic characteristics of the water (i.e., the surface water, groundwater, and Yellow River water); (2) to calculate the river evaporation and investigate the water loss along the flow path of river; (3) to identify the possible sources of evaporated water and determine the relative contribution of multiple recharge sources; and (4) to quantify the influence of the distance to the Yellow River on evaporation and recharge.

Materials and methods

Study area

The study area is located in Dezhou (36°25'–37°58'N, 113°22'–117°83'E), north of the lower reaches of the Yellow River, which belongs to the North China Plain (Fig. 1). Dezhou is bounded by Zhangweixin River in the north and Weiyun River in the west, which respectively close Cangzhou City and Hengshui City. It is also adjacent to Liaocheng City in the southwest and Jinan City in the southeast. This area is strongly affected by a warm temperate semihumid and semiarid climate. The mean air temperature and annual precipitation are 12.9 °C and 547.5 mm (1981–2010) according to the China Meteorological Data Sharing Service System. It is noted that the amount of precipitation from June to September accounts for 75% of the precipitation for the whole year. The mean annual potential evaporation is 1635.7 mm (1981–2010),

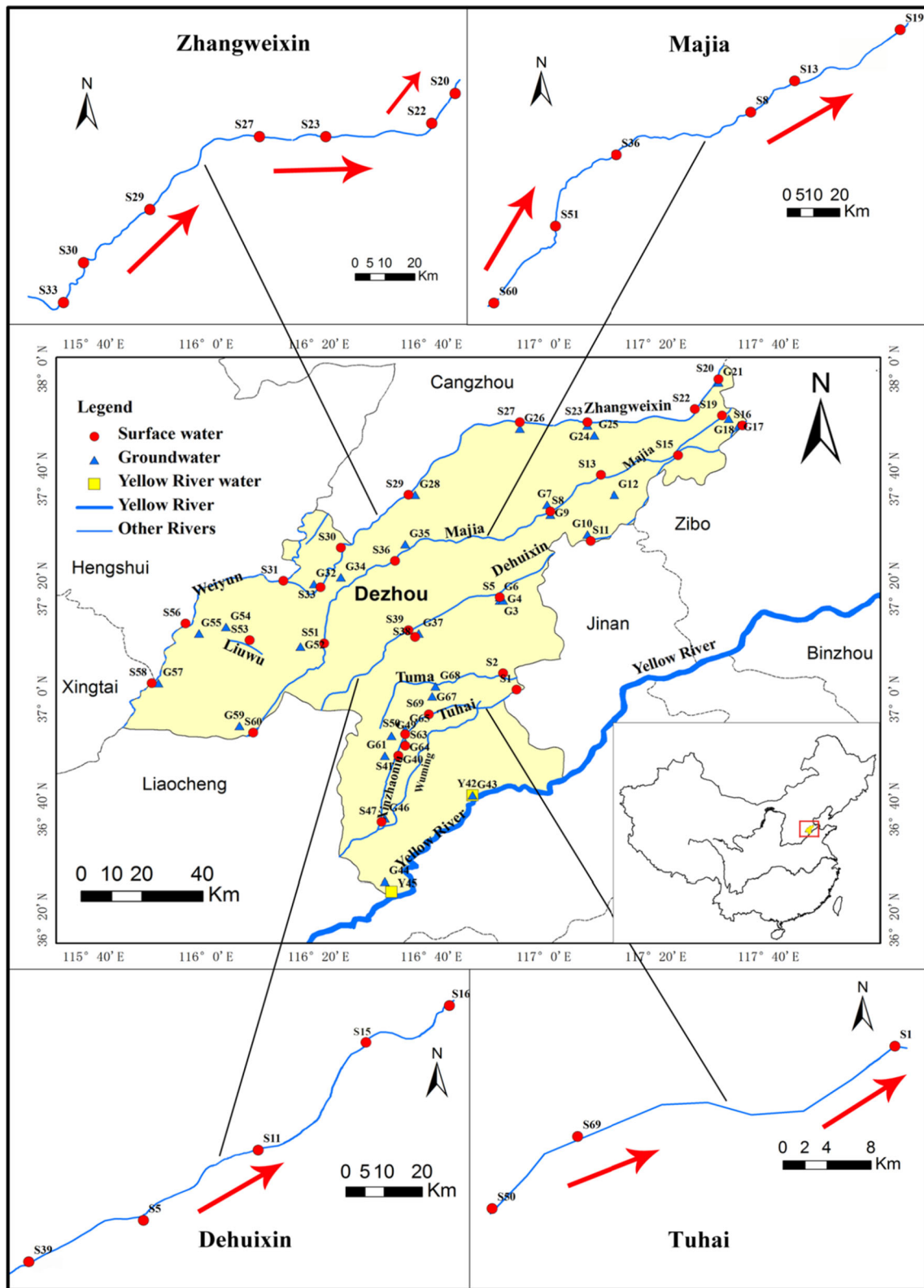


Fig. 1 Location of sampling sites in the lower reaches of the Yellow River. Red arrows denote the flow direction of the rivers

which is lowest (44.8 mm) in December and highest (242.5 mm) in June. The mean river runoff is $6.4 \times 10^8 \text{ m}^3$ (2010) according to the Annual Hydrological Report of China.

As a traditional intensive agricultural area, Dezhou has a farmland of about $4.4 \times 10^5 \text{ hm}^2$ (Wu et al. 2011). The major crops are winter wheat and summer corn. The main rivers include Zhangweixin River, Majia River, Dehuixin River, Tuhai River, Yellow River, and their tributaries, distributing from north to south, flowing through the study area from southwest to northeast. Zhangweixin River and Dehuixin River is originated from Dezhou, Shandong Province, while Majia River and Tuhai River headwaters respectively lie in Puyang, Henan Province and Liaocheng, and Shandong Province. Yellow River is derived from Bayan Har Mountains, Qinghai Province, and finally flows into the Bohai Sea in Shandong Province. The total available water resources including surface water (187 million m^3) and exploitable shallow groundwater resource (434 million m^3) is 621 million m^3 , which is far less than the total water requirement of 2.18 billion m^3 (Sun and Wang 2009). An irrigation project that diverted water from the Yellow River was conducted to largely alleviate this water shortage. Annually, 1.05 billion m^3 of water was diverted from the Yellow River, which accounts for 48.2% of the total amount of the local water resource (Sun and Wang 2009).

Sampling and measurements

The sampling campaigns were carried out in April 2010. Thirty surface water from of ten rivers (the Zhangweixin, Majia, Dehuixin, Tuhai, Xinzhaoniu, Tuma, Weiyun, Zhaowang, Liuwu, and Wuming Rivers) along its flow path following technical regulation of sampling programs (Ministry of Environmental Protection of the People's Republic of China 2009), 33 groundwater from domestic and observation wells (3–70 m) (Yang et al. 2009; Zhang et al. 2014) nearby each surface water sampling site, and two Yellow River water samples were collected. Surface water sampling sites, groundwater sampling sites, and Yellow River water sampling sites were respectively designated as S, G, and Y, which were showed in Fig. 1. Temperature, pH, and electric conductivity (EC) were measured in situ with a portable meter (WM-22EP, DKK-TOA Corporation, Kyoto, Japan). The sampling water was immediately filled into 100-ml high-density polyethylene bottles which were closed tightly to prevent evaporation and contamination and was stored in the refrigerator at 4 °C. Before analysis, all water samples were filtered through 0.45- μm cellulose acetate filter membranes (16,533-Q, Sartorius Stedim Biotech GmbH, Göttingen, Germany).

The $\delta^{18}\text{O}$ and $\delta^2\text{H}$ were analyzed with a liquid water isotope analyzer (Model DLT-100, Los Gatos Research, Mountain View, CA, USA). Each sample was analyzed six times, and the first three results were discarded to minimize the memory effect. The isotopic compositions were reported in standard δ -notation representing ‰ deviations from the Vienna standard mean ocean water standard (V-SMOW). The analytical uncertainty for $\delta^{18}\text{O}$ and $\delta^2\text{H}$ is 0.15 and 0.5‰, respectively.

Model and data calculation

Evaporation calculation model

Rayleigh distillation is the process of phase equilibrium based on an open system. It is assumed that the water–vapor interface is always kept at equilibrium between two phases when evaporation takes place. In addition, the water is fully mixed and ready for evaporation (Wang et al. 2014). Using Rayleigh distillation equation for calculating river evaporation represents the average hydrological characteristics even though a river is a dynamic system (Brooks et al. 2014; Gat 2010). It is noted that infiltration or transpiration might not strongly affect the water's isotopic composition (Dogramaci et al. 2015). Therefore, according to the Rayleigh distillation equation, the evaporation related to isotopic composition can be calculated as follows (Clack and Fritz 1997):

$$R = R_0 f_{\text{re}}^{\varepsilon} \quad (1)$$

where R is the residual isotopic ratio, R_0 is the initial isotopic ratio, f_{re} is the fraction of remaining water, and ε is the fractionation factor, which is calculated as:

$$\varepsilon = \alpha_{v-w} - 1 \quad (2)$$

where α_{v-w} is the equilibrium isotope fractionation factor at the temperature of the vapor–water interface.

The isotopic ratio R in Eq. (1) can also be expressed by isotopic composition δ through the following equation:

$$\begin{aligned} \delta(\text{‰}) &= \frac{R_{\text{sample}} - R_{\text{standard}}}{R_{\text{standard}}} \times 1000 \\ &= \left(\frac{R_{\text{sample}}}{R_{\text{standard}}} - 1 \right) \times 1000 \end{aligned} \quad (3)$$

where R_{sample} is the sample isotopic ratio (e.g., $^{18}\text{O}/^{16}\text{O}$, $^2\text{H}/^1\text{H}$), R_{standard} is the standard isotopic ratio of the V-SMOW reference (3.11×10^4). All mean δ values are mass-weighted.

Substitute Eq. (3) into Eq. (1), and then it can be arranged as:

$$\delta = (\delta_0 + 1000) \times \exp(\varepsilon \times \ln f_{\text{re}}) - 1000 \quad (4)$$

$$f_{\text{ev}} = 1 - f_{\text{re}} \quad (5)$$

where δ_0 is the initial isotopic composition and f_{ev} is the fraction of evaporation water. δ_0 can be obtained by the intersection of the global meteoric water line and local meteoric water line (Wang et al. 2014).

Because fractionation in evaporation involves equilibrium fractionation between the water–vapor and the kinetic fractionation between the vapor–boundary layers in the evaporation interface, the fractionation factor can be stated as:

$$\varepsilon = \varepsilon_{w-v} + \varepsilon_{v-bl} \tag{6}$$

The equilibrium fractionation factor is determined by air temperature (T) and is given by (Majoube 1971):

$$\begin{aligned} \varepsilon_{w-v} &\approx 10^3 \ln \alpha(^{18}O) \\ &= -\frac{1.137 \times 10^6}{T^2} + \frac{0.4156 \times 10^3}{T} + 2.0667 \end{aligned} \tag{7}$$

$$\begin{aligned} \varepsilon_{w-v} &\approx 10^3 \ln \alpha(^2H) \\ &= -\frac{24.844 \times 10^6}{T^2} + \frac{76.248 \times 10^3}{T} - 52.612 \end{aligned} \tag{8}$$

where T is in unites of Kelvin degree. The average air temperature in April 2010 was about 15.2 °C, which is near the average annual air temperature of 15.3 °C during the non-frozen period (1981–2010) in this study area. Thus, 15.2 °C was substituted into Eqs. (7) and (8) and then ε_{w-v} was obtained as -10.17‰ and -86.98‰ for $\delta^{18}O$ and δ^2H , respectively.

Among the factors of surface temperature, wind speed, salinity, and relative humidity that affect kinetic fractionation, relative humidity exerts the most important effect (Clack and Fritz 1997). Gonfiantini (1986) described the kinetic fractionation with relative humidity (h) using the following equations:

$$\varepsilon_{v-bl}(^{18}O) = (h - 1) \times 14.20\text{‰} \tag{9}$$

$$\varepsilon_{v-bl}(^2H) = (h - 1) \times 12.50\text{‰} \tag{10}$$

The relative humidity of 54% in this study area was substituted into Eqs. (9) and (10).

Recharge calculation model

To determine the source and proportion of river recharge, mass conservation was applied as follows:

$$\delta_r = \sum_{i=1}^n P_i \delta_i \tag{11}$$

$$\sum_{i=1}^n P_i = 1 \tag{12}$$

where δ_r represents the isotopic composition of each sampling site in each river, δ_i represents the isotopic

composition of the recharge source, and P_i ($i = 1, 2, \dots, m$) represents the proportion of different recharge sources.

Sensitivity analysis of the evaporation calculation model

To assess the contribution of the input variables (air temperature, relative humidity, and isotopic composition) to the estimated fraction of evaporation and thereby understand the uncertainty of the evaporation model, the sensitivity (S_i) of the estimated fraction of evaporation to each input variable (i) was calculated using the following method (Long and Singh 2012):

$$S_i = \left(\frac{f_{ev\pm} - f_{ev0}}{f_{ev0}} \right) \times 100\% \tag{13}$$

where $f_{ev\pm}$ represents the estimated evaporation fraction when an input variable is increased (+) or decreased (–) with respect to the reference values (original inputs), and f_{ev0} is the estimated fraction of evaporation based on the reference values.

Results and discussion

Isotopic composition of the surface water, groundwater, and Yellow River water

A description of the isotopic composition of water in the hydrological cycle can be traced to Dansgaard (1954) and Craig (1961) and has been interpreted by many researchers (Telmer and Veizer 2000). It can enhance our understanding of the distribution range and frequency of isotopic composition in different water samples, and in estimating the water budget (Tweed et al. 2011). Also, isotopic composition indicates the mixing processes of different water sources and helps to estimate how much water is lost through evaporation (Daessle et al. 2016). Therefore, the stable oxygen and hydrogen isotopic compositions of water samples had first been reported to proceed with the evaporation and recharge calculation. In this study, among the total of 65 samples, 30 were from surface water in rivers, 33 were from groundwater in deep wells, and the two Yellow River water samples were collected in the lower reaches of the Yellow River. The basic characteristics of the different water samples are summarized in Table 1. The isotopic composition in $\delta^{18}O$ and δ^2H of surface water showed a broad range -9.60 to -5.25‰ and -68.5 to -43.3‰ , with an average value of -7.66 and -58.5‰ , respectively. The maximum value of $\delta^{18}O$ was -5.25‰ , derived from site S30 in the Zhangweixin River. Site S2 in the Tuma River produced the minimum value of -9.60‰ . Similar to $\delta^{18}O$, the maximum and minimum value of δ^2H

Table 1 Summary of the temperature, pH, EC, $\delta^{18}\text{O}$, and $\delta^2\text{H}$ of surface water, groundwater, and Yellow River water samples collected in Dezhou, the lower reaches of the Yellow River

Site	Temperature (°C)	pH	EC ($\mu\text{S}/\text{cm}$)	$\delta^{18}\text{O}$ (‰)	$\delta^2\text{H}$ (‰)
S1	9.4	8.2	1220	-8.21	-60.2
S2	7.8	7.7	1616	-9.60	-68.5
S5	9.4	8.3	965	-8.01	-59.9
S8	8.5	8.3	1135	-8.26	-60.3
S11	7.6	8.4	1023	-9.21	-61.3
S13	8.9	8.4	1027	-8.42	-61.9
S15	9.0	8.2	1641	-8.34	-59.1
S16	8.7	8.2	1772	-7.68	-57.5
S19	7.3	8.5	1089	-7.99	-61.5
S20	7.5	8.5	2690	-6.98	-54.3
S22	8.0	8.6	3510	-6.49	-53.7
S23	7.0	8.7	1982	-5.65	-53.1
S27	8.4	8.5	2340	-6.99	-61.1
S29	8.8	8.9	3240	-7.70	-59.5
S30	8.7	8.6	1453	-5.25	-43.3
S31	7.4	8.7	2130	-7.68	-58.5
S33	6.3	9.2	2090	-6.47	-60.2
S36	11.2	8.6	1191	-7.69	-58.4
S38	8.6	8.5	1530	-7.03	-54.4
S39	9.3	7.9	1255	-8.04	-62.6
S41	8.9	8.3	1427	-6.43	-46.8
S47	12.8	8.3	987	-8.75	-62.8
S50	12.9	8.6	998	-7.68	-57.1
S51	11.0	8.4	977	-7.74	-64.9
S53	11.9	8.3	1384	-7.79	-59.7
S56	18.6	9.1	3040	-7.45	-57.1
S58	17.0	8.8	4880	-7.94	-60.1
S60	14.4	9.3	1041	-7.14	-53.1
S63	12.7	7.9	1138	-8.50	-61.8
S69	13.6	8.5	1239	-8.77	-62.4
G3	13.0	7.3	1599	-7.29	-55.3
G4	13.5	7.4	1274	-8.58	-64.1
G6	13.0	7.3	2690	-9.15	-67.8
G7	11.9	7.3	4950	-7.99	-56.0
G9	14.2	7.6	2860	-7.72	-58.9
G10	7.6	8.0	3300	-6.87	-52.0
G12	14.6	7.5	1532	-8.35	-59.1
G17	7.9	7.4	1984	-5.99	-49.6
G18	13.3	7.3	5130	-8.36	-60.6
G21	12.9	7.4	3780	-7.46	-55.9
G24	12.8	7.8	1288	-8.24	-62.7
G25	13.6	7.3	2520	-7.31	-57.5
G26	14.2	7.1	2800	-8.62	-66.3
G28	12.9	7.7	1562	-7.31	-59.2
G32	-	7.2	1990	-7.05	-58.9
G34	14.9	7.3	1323	-9.30	-67.4
G35	13.9	7.5	3250	-8.97	-66.7

Table 1 continued

Site	Temperature (°C)	pH	EC ($\mu\text{S}/\text{cm}$)	$\delta^{18}\text{O}$ (‰)	$\delta^2\text{H}$ (‰)
G37	13.3	7.5	2380	-8.33	-62.0
G40	12.5	7.3	3690	-8.14	-60.1
G43	14.5	7.7	630	-9.53	-65.3
G44	15.5	7.2	1151	-8.89	-65.0
G46	15.2	7.3	1382	-8.33	-63.0
G49	13.4	7.4	1548	-9.44	-66.5
G52	14.7	7.1	2950	-8.50	-63.7
G54	16.2	7.1	4090	-8.15	-60.4
G55	15.4	7.7	3680	-7.87	-57.8
G57	15.0	7.4	1751	-8.07	-64.8
G59	15.2	7.4	1476	-8.69	-63.1
G61	14.3	7.6	843	-8.42	-60.8
G64	13.3	7.4	1776	0.18	-7.4
G65	15.0	7.6	1171	0.26	-8.7
G67	12.5	7.7	1454	-8.14	-59.7
G68	14.7	7.4	2380	-8.11	-58.6
Y42	11.8	8.3	976	-9.27	-64.8
Y45	11.9	8.3	979	-8.88	-64.2

S represents surface water, G represents groundwater, and Y represents the Yellow River water

EC Electrical conductivity

"-" denotes missing value

were -43.3 and -68.5% , which occurred at site S30 in the Zhangweixin River and site S2 in the Tuma River, respectively. The $\delta^{18}\text{O}$ and $\delta^2\text{H}$ values of groundwater ranged from -9.53 to 0.26% and -67.8 to -7.4% , with an average value of -7.66 and -57.7% , respectively. The average $\delta^{18}\text{O}$ and $\delta^2\text{H}$ values of the Yellow River water were -9.08 and -64.5% , respectively.

The global meteoric water line (GMWL) plotted in Fig. 2 represents a regression of $\delta^{18}\text{O}$ and $\delta^2\text{H}$ values from precipitation samples on a global scale (Craig 1961), which can be summarized as $\delta^2\text{H} = 8 \times \delta^{18}\text{O} + 10$. The slope of 8 represents a chemical equilibrium in the water-vapor phase (Jasechko et al. 2013). The isotopic composition of precipitation varies greatly with temporal and spatial variations, which leads to the meteoric water line reflecting the local precipitation characteristic. A slope of less than 8 means a strong kinetic isotope effect influencing evaporation (Jasechko et al. 2013). In this study area, the local meteoric water line (LMWL) was obtained from local precipitation samples and could be expressed as $\delta^2\text{H} = 6.3 \times \delta^{18}\text{O} - 7.45$ with $R^2 = 0.97$ (Zhang et al. 2014). The $\delta^2\text{H}/\delta^{18}\text{O}$ slope was 6.30, driving the isotopic composition of local precipitation below the global meteoric water line. This suggests that this study area was strongly influenced by a semiarid climate. In arid or semiarid climates, non-equilibrium evaporation changes

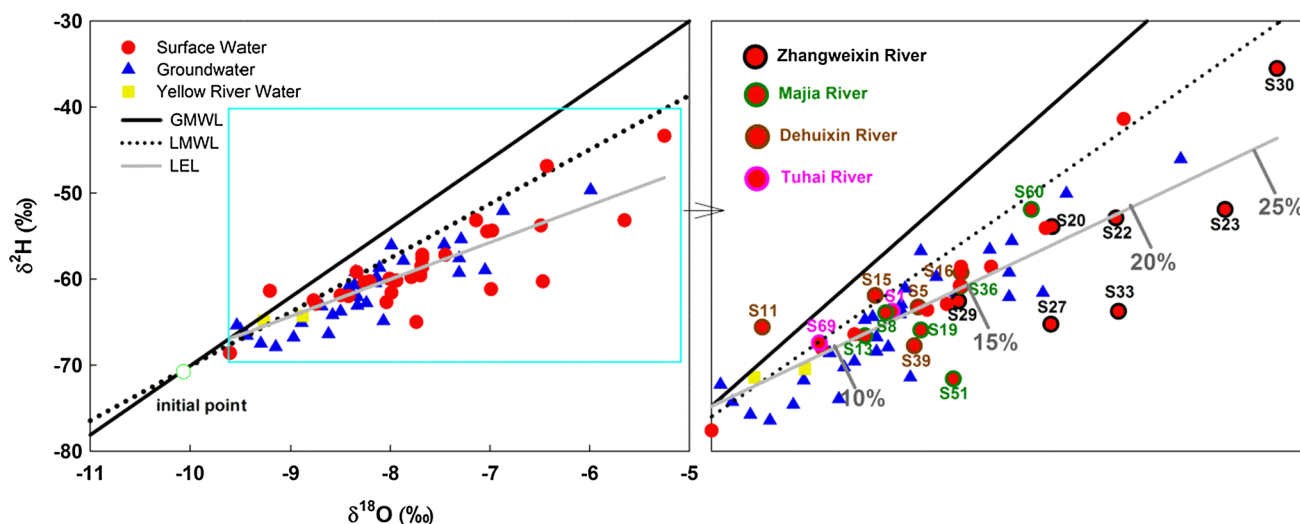


Fig. 2 $\delta^{18}\text{O}$ and $\delta^2\text{H}$ of the surface water, groundwater, and Yellow River water for this study. The red solid circle, blue solid upward triangle, and yellow solid square denote surface water, groundwater, and Yellow River water, respectively. The black solid line, black dotted line, and gray solid line represent the global meteoric water

the isotopic composition, resulting in the river being highly evaporated, which consequently leads to the LMWL deviating from the GMWL (Gibson et al. 2005). Due to evaporation, nearly all the surface water samples fell below the LMWL, except for site S11 in the Dehuixin River where river water might experience re-evaporation. The initial point (−10.26 and −72.1‰) drawn in Fig. 2 was the intersection of the GMWL and LMWL, indicating the beginning of the evaporation (Wang et al. 2014). Meanwhile, it was the most important parameter in the equations used to calculate the evaporation. Surface water was exposed to evaporation and received input waters of similar isotopic composition. It typically distributes along lines in the $\delta^2\text{H}$ - $\delta^{18}\text{O}$ space, defined the local evaporation line (LEL) (Meredith et al. 2009), and could be written as $\delta^2\text{H} = 4.29 \times \delta^{18}\text{O} - 25.61$ with $R^2 = 0.68$ in this study. The LEL intersected with the LMWL, indicating the average isotopic composition of the local water source entering the river prior to evaporation (Dogramaci et al. 2012; Gibson et al. 2005; Jonsson et al. 2009). Also, this intersection provides an input parameter representing the isotopic composition of waters at the catchment scale (Gibson et al. 2005). The obtained GMWL, LMWL, LEL, and two intersections provide detailed hydrological information for future study in this area.

Evaporation of the rivers

To obtain the evaporation proportion, equilibrium and kinetic fractionation factors that relate to the evaporation process were first calculated. The equilibrium fractionation

line (GMWL), local meteoric water line (LMWL), and local evaporation line (LEL), respectively. The initial point (−10.26 and −72.1‰) is the intersection of the GMWL and LMWL. The digits in right sub-figure indicate evaporation proportions of the surface waters

factor is closely related to air temperature. After substituting $T = 15.2$ into Eqs. (7) and (8), then ϵ_{w-v} was obtained as −10.17 and −86.98‰ for $\delta^{18}\text{O}$ and $\delta^2\text{H}$, respectively. The calculation of the kinetic fractionation factor was based on relative humidity of 54% in this study area according to Eqs. (9) and (10). The initial point of evaporation was also plugged into Eq. (4). Through these equations, the evaporation proportions in the rivers were finally obtained as shown in Table 2.

There is a trend of increasing evaporation proportion with isotopic composition (Fig. 3). In other words, the heavier the isotopic composition is, the higher the evaporation proportion is. The average evaporation proportions based on $\delta^{18}\text{O}$ and $\delta^2\text{H}$ of the rivers in this study were both 14.4%. The highest and lowest values for $\delta^{18}\text{O}$ and $\delta^2\text{H}$ were 26.1 and 28.1%, and 3.9 and 4.2%, respectively. In contrast with lakes, rivers receive more recharge sources and run fast, which contributes to evaporation. So, the evaporation proportions of the rivers were lower than the results of lakes in Yinchuan Plain (Qian et al. 2014) and the wastewater reservoir in Baoding (Wang et al. 2014). Also, since meteoric water tends to be more depleted in $\delta^{18}\text{O}$ and $\delta^2\text{H}$ at further inward continent (Dansgaard 1964; Gaj et al. 2015), the result of this study was lower than 35% of dryland river evaporation for Murray River in Australia (Simpson and Herczeg 1991).

Different rivers exhibit different evaporation proportions due to the unique river characteristics. In this study, the mean evaporation proportion of ten rivers (the Zhangweixin, Majia, Dehuixin, Tuhai, Xinzhaoni, Tuma, Weiyun, Zhaowang, Liuwu, and Wuming Rivers) were

Table 2 Calculated evaporation proportions for rivers in the lower reaches of the Yellow River

Rivers	Calculated evaporation proportion (%)			
	Site	$f_{ev}(\delta^{18}O)$	$f_{ev}(\delta^2H)$	$f_{ev}(\text{average})$
Zhangweixin River	S33	20.5	12.9	16.7
	S30	26.1	28.1	27.1
	S29	14.3	13.6	14.0
	S27	17.9	12.0	15.0
	S23	24.3	19.7	22.0
	S22	20.4	19.1	19.8
	S20	18.0	18.5	18.3
	Average	20.2	17.7	19.0
Majia River	S60	17.2	19.7	18.5
	S51	14.1	8.1	11.2
	S36	14.4	14.7	14.6
	S8	11.4	12.8	12.1
	S13	10.5	11.1	10.9
	S19	12.8	11.6	12.3
	Average	13.4	13.0	13.2
Dehuixin River	S39	12.6	10.4	11.5
	S5	12.7	13.1	12.9
	S11	6.2	11.8	9.0
	S15	11.0	14.0	12.5
	S16	14.4	15.6	15.1
Tuhai River	Average	11.4	13.0	12.2
	S50	14.4	15.9	15.2
	S69	8.6	10.6	9.7
	S1	11.7	12.9	12.3
Xinzhaoniu River	Average	11.6	13.1	12.4
	S47	8.7	10.2	9.5
	S41	20.6	25.2	23.0
Tuma River	Average	14.7	17.7	16.2
	S2	3.9	4.2	4.1
Weiyun River	S31	14.4	14.5	14.5
	S56	15.6	15.9	15.8
	S58	13.1	13.0	13.1
Zhaowang River	Average	14.4	14.5	14.5
	S38	17.7	18.5	18.1
Liuwu River	S53	13.9	13.3	13.6
Wuming River	S63	10.1	11.3	10.7
Average		14.4	14.4	14.4

19.0, 13.2, 12.2, 12.4, 16.2, 4.1, 14.5, 18.1, 13.6, and 10.7%, respectively. Due to its narrow and short (21.4 km) river channel, the evaporation proportion of the Tuma River was the lowest among the all rivers. The Zhangweixin River had the highest evaporation proportion, because the Zhangweixin River is relatively long (151 km) and therefore experiences a much greater evaporative loss. Among the main rivers in this study area, the Majia River

and Tuhai River are both broad and straight (Liu 2007), which results in a relatively small range of fluctuation in the evaporation proportion. The average evaporation proportion of the westernmost sampling site (S39) for the Dehuixin River was 11.5%, which was lower than the westernmost sampling sites in the other three rivers (site S33 in the Zhangweixin River: 16.7%, site S60 in the Majia River: 18.5%, and site S50 in the Tuhai River: 15.2% as shown in Table 2). This can be attributed to the shortest distance from site S39 to its source of the Dehuixin river, and at which the evaporation actually is little (Qian et al. 2007; Wang et al. 2014). In addition, the Dehuixin River is artificially dug and is subject to anthropogenic influences such as drainage and flood control (Liu 2007), which leads to variations of water volume and therefore less evaporation.

Evaporation along the river flow path

Isotopic compositions have a linear increasing trend with increasing distance along the channel on the condition that evaporation predominates (Wang et al. 2014). To test the evaporation proportions whether or not increase with the flow path along rivers, each main river was considered as one unit, and then the river was divided into several cells according to the sampling site. Sampling site was set from west to east along the flow path in each main river. The westernmost sampling site was considered to be the starting point when calculating the distance. The distance was measured from starting point (westernmost sampling site) to each sampling site. From Fig. 4, it was clear that evaporation proportions of the sampling sites for the four main rivers (the Zhangweixin, Majia, Dehuixin, and Tuhai Rivers) fluctuated along the flow path. Along the Zhangweixin River, from site S30 to S29, the evaporation proportion displayed a significant decreasing trend, and then increased from site S29, but decreased at sites S22 and S20 consecutively. Similar to the Zhangweixin River, the Majia River also decreased at three sites, S51, S8, and S13, respectively. Different from the Zhangweixin River, the evaporation of the Majia River decreased as a whole. Dehuixin River's evaporation gradually increased along the flow path except at site S11. Site S69's evaporation in the Tuhai River was significantly lower than that of sampling sites S1 and S50.

Among the factors leading to the result that the evaporation proportion does not closely follow an increasing trend along the flow path, recharge might be the most significant influential factor. As shown in Table 3 (data source and calculation process were discussed in next section), site S29 in the Zhangweixin River, sites S51, S8, and S13 in the Majia River, site S11 in the Dehuixin River, and site S69 in the Tuhai River all received recharge by

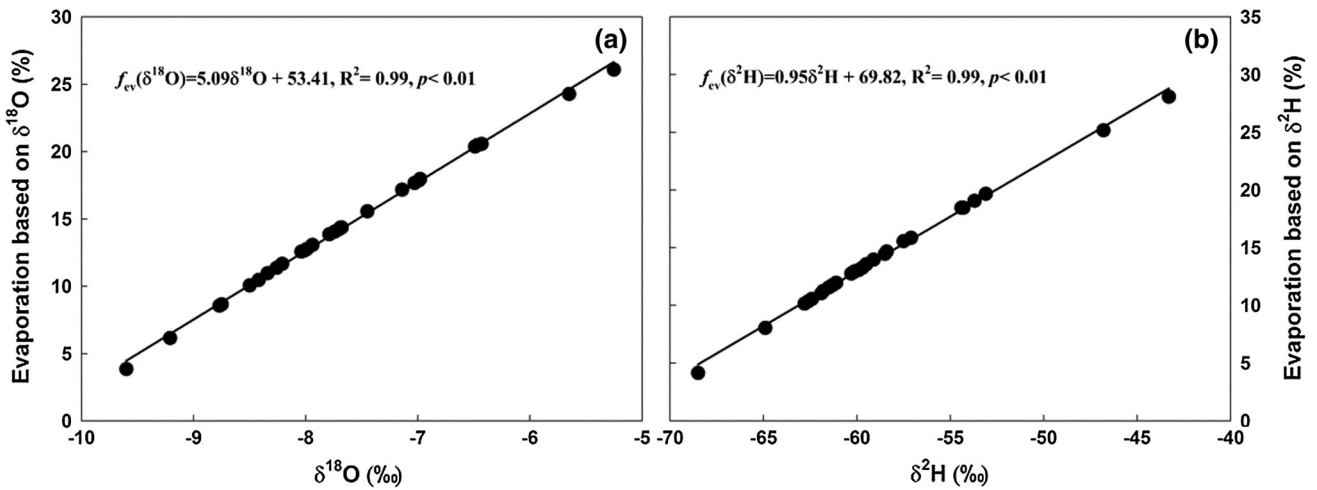


Fig. 3 Relationship of the isotopic composition based on $\delta^{18}\text{O}$ (a) and $\delta^2\text{H}$ (b) with evaporation proportion. The solid line ($f_{\text{ev}}(\delta^{18}\text{O}) = 5.09\delta^{18}\text{O} + 53.41$, $R^2 = 0.99$, $p < 0.01$) (a) and ($f_{\text{ev}}(\delta^2\text{H}) = 0.95\delta^2\text{H} + 69.82$, $R^2 = 0.99$, $p < 0.01$) (b) indicates the linear trend of the isotopic composition and evaporation proportion, respectively

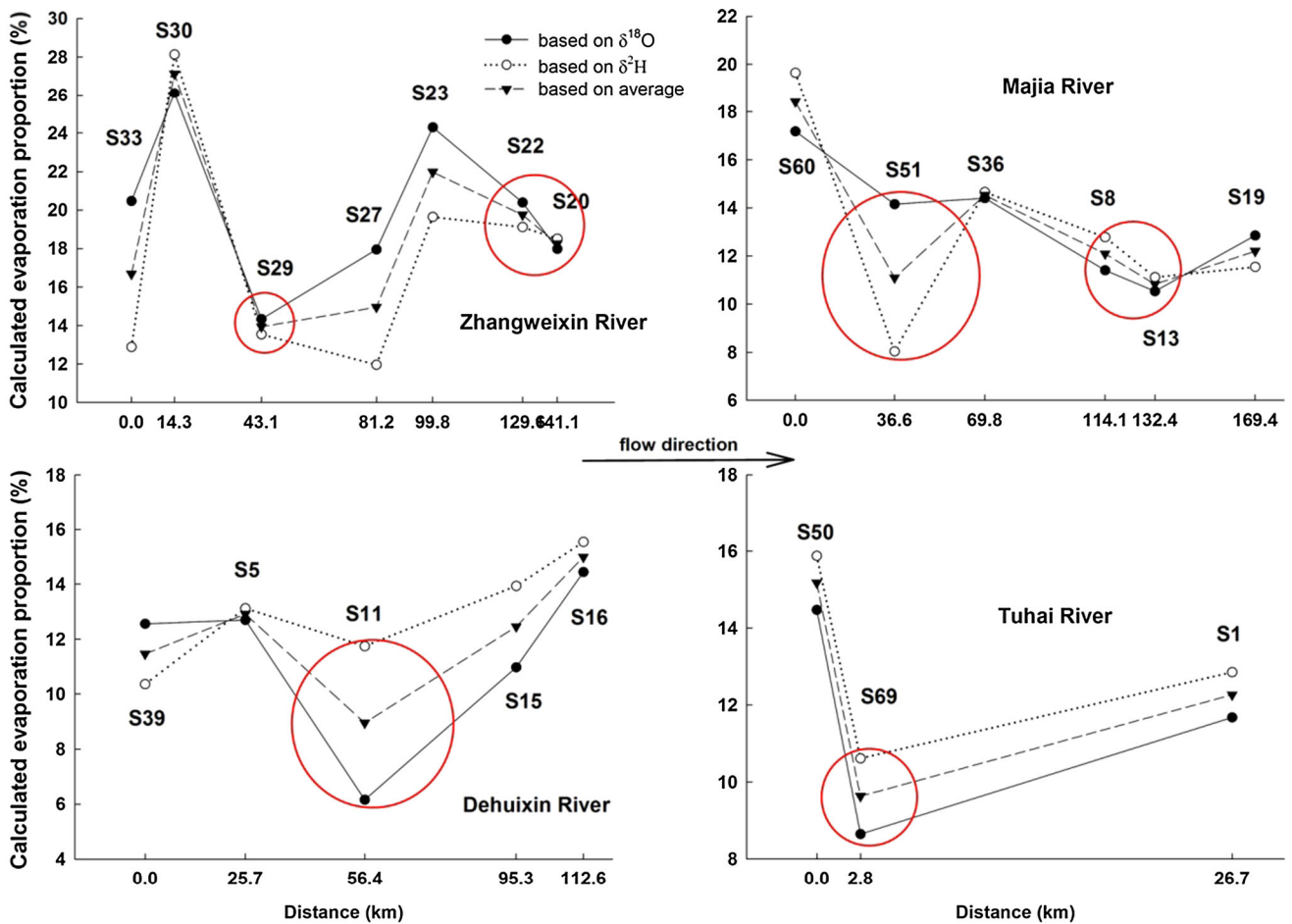


Fig. 4 Variation of evaporation proportions in the four main rivers (the Zhangweixin, Majia, Dehuixin, and Tuhai Rivers) along the flow path in the lower reaches of the Yellow River. The black solid circle, open circle, and down-triangle denote the evaporation proportion calculated based on $\delta^{18}\text{O}$, $\delta^2\text{H}$, and their average, respectively. The

red circle indicates the sampling site that did not follow the increasing trend of evaporation along the flow path. Distance, the horizontal axis title, denote the distance between each sampling site and the westernmost sampling site along the flow path in each river

other water sources. As for sites S22 and S20 in Zhangweixin River and site S11 in the Dehuixin River, other factors such as salinity and flow rate might result in this decrease in evaporation along the flow path. Researchers have documented that large increases in salinity would not accompany heavy isotope enrichment (Paces and Wurster 2014; van den Akker et al. 2011), whereas most of this heavy isotope enrichment is the result of evaporation. In the Zhangweixin River, site S22 exhibits the relatively high EC value of 3510 $\mu\text{S}/\text{cm}$ (Table 1), which therefore adverse to evaporation. Since high flow velocity would decrease the evaporation (Qian et al. 2007), the evaporation proportions of site S20 in the Zhangweixin River and site S11 in the Dehuixin River were lower.

Recharge source and proportion

As described in the preceding section, recharge might be the most prevalent among the factors in this study area and may have significantly changed the river isotopic composition. Consequently, the river evaporation proportions did not increase along the flow path. Evaporation and recharge change the river isotopic composition at the opposite trend. The process of evaporation drives the increase of the isotopic composition, while the recharge process makes it decrease (Qian et al. 2007). It is difficult to quantify distinct mixing end members because contributions from

different water sources are affected by complex hydrologic settings (Paces and Wurster 2014). Precipitation, groundwater, and Yellow River water are commonly considered to be the important water sources (Li et al. 2008). Henderson and Shuman (2010) noted that precipitation exerts less influence on the isotopic composition of rivers than lakes. Since little precipitation falls around April in this area, local precipitation recharge was ignored in this study. Groundwater recharge is a key component in a semiarid area (Dogramaci et al. 2012). The Yellow River flows from southwest to northeast through this area, and exerts a strong influence on the local water cycle. Furthermore, river water had a close hydraulic relationship with groundwater and Yellow River water, as shown in Fig. 2. Above all, Yellow River water and groundwater jointly recharged the rivers in this area. It is noted that precipitation should serve as a recharge source for rivers in wet season because it changes the water isotopic composition. Therefore, further studies on recharge estimation might be paid more attention to its differences resulting from sampling in different seasons.

Recharge proportions were estimated based on a mass conservation model. According to Eqs. (11) and (12), δ_r is the isotopic composition at each sampling site in each river. $\delta_i (i = 1, 2, \dots, m)$ is the isotopic composition of the recharge source. In this study, $m = 2$, δ_1 and δ_2 are the isotopic composition of Yellow River water and groundwater, respectively. $\delta^{18}\text{O}$ and $\delta^2\text{H}$ in averaged groundwater

Table 3 Calculated recharge proportions based on $\delta^{18}\text{O}$ for rivers in the lower reaches of the Yellow River

Rivers	Site	Distance to the Yellow River (km)	Calculated recharge proportion (%) Yellow River	Groundwater
Zhangweixin River	S29	94.1	3.1	96.9
	S22	70.7	–	–
	S20	78.8	–	–
Weiyun River	S31	105	1.2	98.8
	S58	92.6	19.8	80.2
Majia River	S51	64.7	5.6	94.4
	S36	101.4	2.2	97.8
	S8	79.1	42.4	57.6
	S13	69.3	53.8	46.2
	S19	67.0	23.2	76.8
Dehuixin River	S39	60.9	27.0	73.0
	S5	55.3	25.1	74.9
	S11	68.6	–	–
Tuhai River	S15	62.5	47.9	52.1
	S69	40.0	78.1	21.9
Wuming River	S1	27.4	38.7	61.3
	S63	25.2	59.3	40.7
Xinzhaoni River	S47	26.1	77.3	22.7

Bold font in rivers denotes the main rivers in this area. Bold font in site means that the sampling site did not follow the increasing trend of evaporation along the flow path. Sampling sites in each river are arranged along the flow path in sequence. “–” represent the sampling site received no recharge from the two sources

from 33 samples and averaged Yellow River water from two samples are considered to be the isotopic composition of the recharge source. The average $\delta^{18}\text{O}$ and $\delta^2\text{H}$ of Yellow River water are -9.08 and -64.5‰ , and those of groundwater are -7.66 and -57.7‰ , respectively. P_1 and P_2 are the recharge proportion of Yellow River water and groundwater, respectively. The calculated recharge proportions for rivers are displayed in Table 3.

It showed that the recharge source could be divided into three groups (Table 3). Sampling sites such as S29 in the Zhangweixin River; S51, S36, and S19 in the Majia River; S39 and S5 in the Dehuixin River; S31 and S58 in the Weiyun River; and S1 in the Tuhai River were mainly recharged by groundwater. Their recharge proportions were about 96.9, 94.4, 97.8, 76.8, 73.0, 74.9, 98.8, 80.2, and 61.3%, respectively. The second group was mainly fed by Yellow River water: 78.1% of site S69 in the Tuhai, 59.3% of site S63 in the Wuming River and 77.3% of site S47 in the Xinzhaoni River were mainly recharged by Yellow River water. Other sampling sites were mixed recharged by Yellow River water and groundwater. The recharge proportion of Yellow River water and groundwater in site S8 of the Majia River were 42.4 and 57.6%, and those of site S13 of the Majia River were 53.8 and 46.2%, respectively. Site S15 in the Dehuixin River received 47.9 and 52.1% recharge from Yellow River water and groundwater, respectively. Furthermore, it was found that the recharge from Yellow River increased while that from groundwater decreased with the increase in the distance to the Yellow River. The variations in the recharge proportions could be attributed to the river's spatial distributions (i.e., the differences in the distance to the Yellow River). From Fig. 1, the Zhangweixin, Weiyun, Majia, Dehuixin, Tuhai, Wuming, Xinzhaoni, and Yellow Rivers distribute from north to south in sequence.

How the distance to the Yellow River affects evaporation and recharge

The Yellow River plays a critical role in regulating hydrological processes including evaporation and recharge in this study area. Figure 5a and b respectively depicted the relationship between evaporation/recharge proportion and the distance to the Yellow River. Figure 5a showed that evaporation increased with an increase in the distance to the Yellow River, while Fig. 5b suggested that recharge decreased with an increase in the distance to the Yellow River. This indicated that the influences of the distance to the Yellow River on evaporation and recharge are governed by opposite processes.

The three regression equations presented in Fig. 5a represented the relationship between evaporation proportion with the distance to the Yellow River based on $\delta^{18}\text{O}$, $\delta^2\text{H}$, and their average, respectively. The slopes of each regressions ($0.102^* \pm 0.042$, 0.079 ± 0.040 , and $0.090^* \pm 0.038$) (Slope^{significant} \pm standard error, *Significant trend at the 95% confidence level, **Significant trend at the 99% confidence level) indicated the change rate of the evaporation proportion with the distance to the Yellow River. The evaporation proportion averaged increased by 1.02, 0.79, 0.90% per increase of 10 km farther away from the Yellow River based on $\delta^{18}\text{O}$, $\delta^2\text{H}$, and their average, respectively. The relationship between the evaporation proportion with distance to the Yellow River based on $\delta^2\text{H}$ was insignificant due to its higher p value of regression ($p > 0.05$) compared with $\delta^{18}\text{O}$ and their average. The regression based on $\delta^{18}\text{O}$ and their average were significant ($p < 0.05$) and therefore more reliable.

The relationship between the recharge proportion by the Yellow River and the distance to the Yellow River is displayed as three regression equations based on $\delta^{18}\text{O}$, $\delta^2\text{H}$,

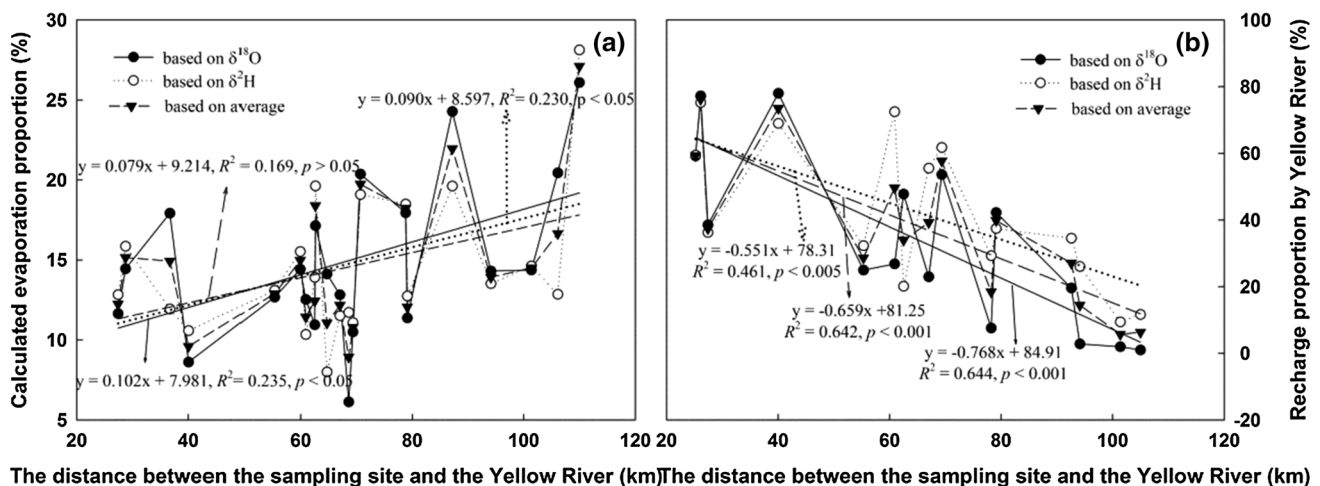


Fig. 5 Relationship between evaporation proportions (a) and recharge proportions (b) with the distance from sampling site to the Yellow River. The black solid, dotted, and dashed lines denote linear trend based on $\delta^{18}\text{O}$, $\delta^2\text{H}$, and their average, respectively

and their average, respectively in Fig. 5b. The slopes of the three regressions were respectively $-0.768^{**} \pm 0.158$, $-0.551^{**} \pm 0.165$, and $-0.659^{**} \pm 137$ (Slope^{significant} \pm standard error, *Significant trend at the 95% confidence level, **Significant trend at the 99% confidence level), indicating that the recharge proportion averaged decreased by 7.68, 5.51, and 6.59% per increase of 10 km farther away from the Yellow River based on $\delta^{18}\text{O}$, $\delta^2\text{H}$, and their average, respectively. Similar to the evaporation process, the result based on $\delta^{18}\text{O}$ was more predictable than that based on $\delta^2\text{H}$ as suggested by the higher R^2 (0.644 vs. 0.461).

The fitted empirical equations might offer a new way to quantify the spatial effect of the Yellow River on evaporation and recharge. Compared with evaporation, recharge was more easily affected by the distance to the Yellow River due to the greater change rate and the higher significance. This result contributes to quantify the effect of the Yellow River on hydrological processes. In addition, using $\delta^{18}\text{O}$ was more reliable than $\delta^2\text{H}$ in exploring the relationship of the evaporation and recharge with the distance to the Yellow River.

Sensitivity analysis of the evaporation calculation model

Sensitivity analysis was performed according to Eq. (13). In this study, input variables (i) including air temperature (T), relative humidity (h), and isotopic composition (δ) in this equation drive the variations of the evaporation. The variation steps of T and h were 0.5 °C and 0.05, respectively. The variation steps of δ was based on the analytical uncertainty of $\delta^{18}\text{O}$ (0.15‰) and $\delta^2\text{H}$ (0.5‰).

Figure 6a showed that T and h were positively correlated with the evaporation proportion. A 0.5 °C (equally, a 3% relative change) increase in T could result in a 0.2% (denoted as relative change in evaporation proportion) increase in evaporation proportion. A 0.05 (equally, a 9% relative change) increase in h could result in a 4% increase in the evaporation proportion. Conversely, a 0.15‰ (equally, a -2% relative change) increase in $\delta^{18}\text{O}$ could result in a 6% decrease in evaporation proportion. This meant that the estimated evaporation proportion based on $\delta^{18}\text{O}$ is more sensitive to δ than T and h .

As for $\delta^2\text{H}$, Fig. 6b shows that T and h were positively correlated with evaporation proportion, but δ was negatively correlated with evaporation proportion. A 0.5 °C (equally, a 3% relative change) increase in T could result in a 0.6% (denoted as relative change in evaporation proportion) increase in the evaporation proportion. A 0.05 (equally, 9% relative change) increase in h could result in a 0.6% increase in evaporation proportion. A 0.5‰ (equally, a -0.9% relative change) increase in $\delta^2\text{H}$ could result in a 4% decrease in the evaporation proportion. Likewise, the estimated evaporation proportion is more sensitive to δ than T and h .

It is noted that a variation in h could have more prominent effects on the evaporation proportion based on $\delta^{18}\text{O}$ than $\delta^2\text{H}$, whereas T might exert a greater influence on the evaporation based on $\delta^2\text{H}$ rather than $\delta^{18}\text{O}$. Temperature and relative humidity accuracy depends on the meteorological station distribution. The measured deviation or extreme weather could trigger a larger calculation error (Skrzypek et al. 2015). In fact, the evaporation proportion was most sensitive to isotopic composition when comparing meteorological variables.

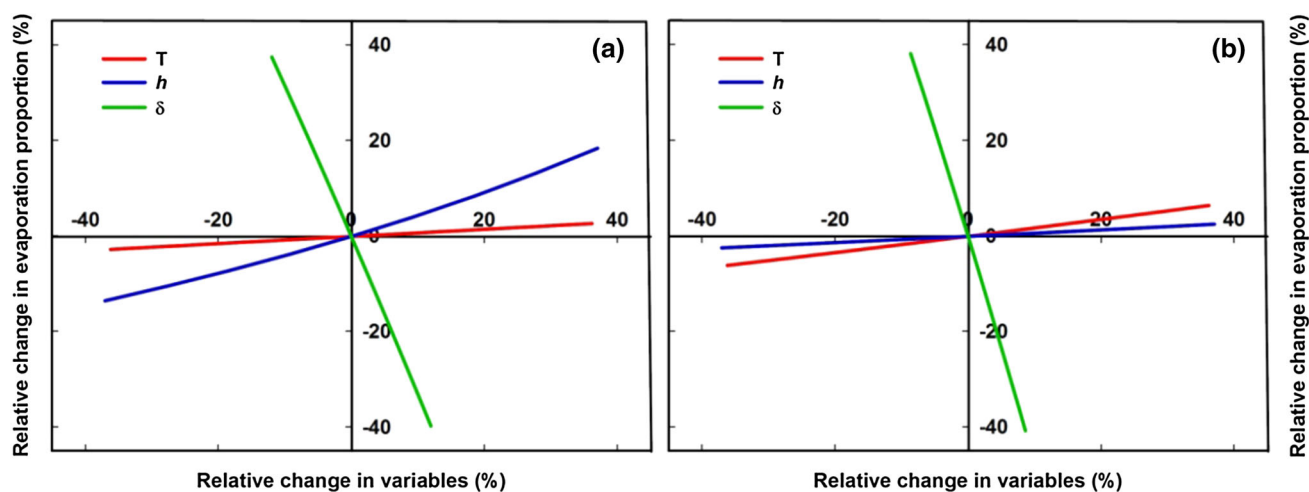


Fig. 6 Sensitivity analysis of evaporation proportion based on $\delta^{18}\text{O}$ (a), $\delta^2\text{H}$ (b) to air temperature (T), relative humidity (h), and isotopic composition (δ). Variations of T are specified between 9.7 and 20.7 °C, with a variation step of 0.5 °C. Variations of h are specified

between 0.34 and 0.74, with a variation step of 5%. The variation step of δ based on $\delta^{18}\text{O}$ is 0.15‰. The variation step of δ based on $\delta^2\text{H}$ is 0.5‰

Therefore, minor variations in isotopic composition would lead to large uncertainty in evaporation proportion estimates. In addition, the initial isotopic composition δ_0 is also an input variable, which this study did not focus on because it is derived from the intersection of the GMWL and LMWL. This sensitivity analysis is critical for choosing an appropriate isotope type when data are limited and for controlling analytical uncertainty of the isotopic composition to ensure an accurate estimation the evaporation proportion.

Conclusions

This study showed that the $\delta^{18}\text{O}$ and $\delta^2\text{H}$ of the rivers in the lower reaches of the Yellow River were strongly influenced by evaporation. According to the Rayleigh distillation equation, the evaporation proportion of the rivers were both averaged 14.4% with a range from 3.9 to 26.1%, and 4.2 to 28.1% based on $\delta^{18}\text{O}$ and $\delta^2\text{H}$, respectively. Mainly due to the effects of recharge, the evaporation proportion along the flow path did not show a linear increasing trend. Yellow River water and groundwater, as the main recharge sources in dry season, supplied the rivers at different proportions and consequently different groups. Opposite trends were found in evaporation and recharge proportions with the distance to the Yellow River. With per 10-km increases far away from the Yellow River, evaporation proportions increased by 1.02, 0.79, and 0.90% while recharge proportions decreased by 7.68, 5.51, and 6.59% based on $\delta^{18}\text{O}$, $\delta^2\text{H}$, and their average, respectively. Based on the statistical analyses, using $\delta^{18}\text{O}$ was more reliable than $\delta^2\text{H}$ for investigating the spatial influence of the Yellow River on evaporation and recharge.

Acknowledgements We are greatly thankful to Jing Li, Chun Tu, Qiang Liu, Yan Zhang, Shuai Song for their help with field and laboratory assistance. This study was supported by the National Natural Science Foundation of China No. 41271047, the National Key Research and Development Program of China (2016YFD0800301), and the National Key Technology R&D Program of China (2012BAD05B0204).

References

Brooks JR, Gibson JJ, Birks SJ, Weber MH, Rodecap KD, Stoddard JL (2014) Stable isotope estimates of evaporation: inflow and water residence time for lakes across the United States as a tool for national lake water quality assessments. *Limnol Oceanogr* 59:2150–2165. doi:10.4319/lo.2014.59.6.2150

Chen JS, He DW, Cui SB (2003) The response of river water quality and quantity to the development of irrigated agriculture in the last 4 decades in the Yellow River Basin, China. *Water Resour Res*. doi:10.1029/2001wr001234

Clack I, Fritz P (1997) *Environmental isotopes in hydrogeology*. CRC Press, New York

Craig H (1961) Isotopic variations in meteoric waters. *Science* 133:1702–1703. doi:10.1126/science.133.3465.1702

Daessle LW, Van Geldern R, Orozco-Duran A, Barth JAC (2016) The 2014 water release into the arid Colorado River delta and associated water losses by evaporation. *Sci Total Environ* 542:586–590. doi:10.1016/j.scitotenv.2015.09.157

Daniel CC (2015) River evaporation, condensation and heat fluxes within a first order tributary of Catamaran Brook (New Brunswick, Canada). *Hydrol Process* 30(12):1872–1883. doi:10.1002/hyp.10744

Dansgaard W (1954) The O^{18} abundance in fresh water. *Geochim Cosmochim Acta* 6:241–260. doi:10.1016/0016-7037(54)90003-4

Dansgaard W (1964) Stable isotopes in precipitation. *Tellus* 16:436–468

Dogramaci S, Skrzypek G, Dodson W, Grierson PF (2012) Stable isotope and hydrochemical evolution of groundwater in the semi-arid Hamersley Basin of subtropical northwest Australia. *J Hydrol* 475:281–293. doi:10.1016/j.jhydrol.2012.10.004

Dogramaci S, Firmani G, Hedley P, Skrzypek G, Grierson PF (2015) Evaluating recharge to an ephemeral dryland stream using a hydraulic model and water, chloride and isotope mass balance. *J Hydrol* 521:520–532. doi:10.1016/j.jhydrol.2014.12.017

Elmi G, Sacchi E, Zuppi GM, Cerasuolo M, Allais E (2013) Isotopic estimation of the evapo-transpiration flux in a plain agricultural region (Po plain, Northern Italy). *Appl Geochem* 34:53–64. doi:10.1016/j.apgeochem.2012.12.010

Ershadi A, McCabe MF, Evans JP, Chaney NW, Wood EF (2014) Multi-site evaluation of terrestrial evaporation models using FLUXNET data. *Agric For Meteorol* 187:46–61. doi:10.1016/j.agrformet.2013.11.008

Gaj M, Beyer M, Koeniger P, Wanke H, Hamutoko J, Himmelsbach T (2015) In-situ unsaturated zone stable water isotope (^2H and ^{18}O) measurements in semi-arid environments using tunable off-axis integrated cavity output spectroscopy. *Hydrol Earth Syst Sci Discuss* 12:6115–6149. doi:10.5194/hessd-12-6115-2015

Gat J (2010) *Stable isotopes of fresh and saline lakes. Isotope hydrology: a study of the water cycle*. Imperial College Press, London

Gibson JJ, Edwards TWD (2002) Regional water balance trends and evaporation-transpiration partitioning from a stable isotope survey of lakes in northern Canada. *Glob Biogeochem Cycles* 16:1026. doi:10.1029/2001gb001839

Gibson JJ, Edwards TWD, Bursey GG, Prowse TD (1993) Estimating evaporation using stable isotopes: quantitative results and sensitivity analysis for two catchments in northern Canada. *Nord Hydrol* 24:79–94

Gibson JJ et al (2005) Progress in isotope tracer hydrology in Canada. *Hydrol Process* 19:303–327. doi:10.1002/hyp.5766

Gonfiantini R (1986) Environmental isotopes in lake studies. In: Fritz P, Fontes J-Ch (eds) *Handbook of environmental isotope geochemistry. The terrestrial environment*. Elsevier, Amsterdam

Henderson AK, Shuman BN (2010) Differing controls on river- and lake-water hydrogen and oxygen isotopic values in the western United States. *Hydrol Process* 24:3894–3906. doi:10.1002/hyp.7824

Hostetler SW, Bartlein PJ (1990) Simulation of lake evaporation with application to modeling lake level variations of Harney-Malheur lake, Oregon. *Water Resour Res* 26:2603–2612. doi:10.1029/WR026i010p02603

Jasechko S, Sharp ZD, Gibson JJ, Birks SJ, Yi Y, Fawcett PJ (2013) Terrestrial water fluxes dominated by transpiration. *Nature* 496:347–351. doi:10.1038/nature11983

- Jonsson CE, Leng MJ, Rosqvist GC, Seibert J, Arrowsmith C (2009) Stable oxygen and hydrogen isotopes in sub-Arctic lake waters from northern Sweden. *J Hydrol* 376:143–151. doi:[10.1016/j.jhydrol.2009.07.021](https://doi.org/10.1016/j.jhydrol.2009.07.021)
- Krabbenhoft DP, Bowser CJ, Anderson MP, Valley JW (1990) Estimating groundwater exchange with lakes. 1. The stable isotope mass balance method. *Water Resour Res* 26:2445–2453. doi:[10.1029/90wr01135](https://doi.org/10.1029/90wr01135)
- Li F, Pan G, Tang C, Zhang Q, Yu J (2008) Recharge source and hydrogeochemical evolution of shallow groundwater in a complex alluvial fan system, southwest of North China Plain. *Environ Geol* 55:1109–1122. doi:[10.1007/s00254-007-1059-1](https://doi.org/10.1007/s00254-007-1059-1)
- Li Q, Nakatsuka T, Kawamura K, Liu Y, Song HM (2011) Hydroclimate variability in the North China Plain and its link with El Niño-Southern Oscillation since 1784 A.D.: Insights from tree-ring cellulose $\delta^{18}\text{O}$. *J Geophys Res*. doi:[10.1029/2011JD015987](https://doi.org/10.1029/2011JD015987)
- Liu T (2007) Study on the present condition and variety regulation of binzhou water environment. Thesis, Hehai University
- Liu Y, Zhang XJ, Song HM, Cai QF, Li Q, Zhao BY, Liu H, Mei RC (2016) Tree-ring-width-based PDSI reconstruction for central Inner Mongolia, China over the past 333 years. *Clim Dyn*. doi:[10.1007/s00382-016-3115-6](https://doi.org/10.1007/s00382-016-3115-6)
- Long D, Singh VP (2012) A two-source trapezoid model for evapotranspiration (TTME) from satellite imagery. *Remote Sens Environ* 121:370–388. doi:[10.1016/j.rse.2012.02.015](https://doi.org/10.1016/j.rse.2012.02.015)
- Maheu A, Caissie D, St-Hilaire A, El-Jabi N (2014) River evaporation and corresponding heat fluxes in forested catchments. *Hydrol Process* 28:5725–5738. doi:[10.1002/hyp.10071](https://doi.org/10.1002/hyp.10071)
- Majoube M (1971) Fraction in O-18 between ice and water vapor. *J Chim Phys Phys Chim Biol* 68:625
- McCallum AM, Andersen MS, Acworth RI (2014) A new method for estimating recharge to unconfined aquifers using differential river gauging. *Groundwater* 52:291–297. doi:[10.1111/gwat.12046](https://doi.org/10.1111/gwat.12046)
- Meredith KT, Hollins SE, Hughes CE, Cendón DI, Hankin S, Stone DJM (2009) Temporal variation in stable isotopes (^{18}O and ^2H) and major ion concentrations within the Darling River between Bourke and Wilcannia due to variable flows, saline groundwater influx and evaporation. *J Hydrol* 378:313–324. doi:[10.1016/j.jhydrol.2009.09.036](https://doi.org/10.1016/j.jhydrol.2009.09.036)
- Ministry of Environmental Protection of the People's Republic of China (2009) Water quality-Technical regulation on the design of sampling programmes (HJ 495-2009). Standards of the People's Republic of China on Environmental Protection
- Paces JB, Wurster FC (2014) Natural uranium and strontium isotope tracers of water sources and surface water-groundwater interactions in arid wetlands—Pahrnagat Valley, Nevada, USA. *J Hydrol* 517:213–225. doi:[10.1016/j.jhydrol.2014.05.011](https://doi.org/10.1016/j.jhydrol.2014.05.011)
- Palmer PC, Gannett MW, Hinkle SR (2007) Isotopic characterization of three groundwater recharge sources and inferences for selected aquifers in the upper Klamath Basin of Oregon and California, USA. *J Hydrol* 336:17–29. doi:[10.1016/j.jhydrol.2006.12.008](https://doi.org/10.1016/j.jhydrol.2006.12.008)
- Qian H, Li M, Ji Y, Yang B, Zhao Z (2007) Changes of $\delta^{18}\text{O}$ and δD along the Dousitu River, Inner Mongolia, China, and their evidence of river water evaporation. *Aquat Geochem* 13:127–142
- Qian H, Wu J, Zhou Y, Li P (2014) Stable oxygen and hydrogen isotopes as indicators of lake water recharge and evaporation in the lakes of the Yinchuan Plain. *Hydrol Process* 28:3554–3562. doi:[10.1002/hyp.9915](https://doi.org/10.1002/hyp.9915)
- Richey JE, Hedges JI, Devol AH, Quay PD, Victoria R, Martinelli L, Forsberg BR (1990) Biogeochemistry of carbon in the Amazon river. *Limnol Oceanogr* 35:352–371
- Shen Y, Zhang Y, Scanlon BR, Lei H, Yang D, Yang F (2013) Energy/water budgets and productivity of the typical croplands irrigated with groundwater and surface water in the North China Plain. *Agric For Meteorol* 181:133–142. doi:[10.1016/j.agrfor.2013.07.013](https://doi.org/10.1016/j.agrfor.2013.07.013)
- Simpson HJ, Herczeg AL (1991) Stable isotopes as an indicator of evaporation in the river Murray, Australia. *Water Resour Res* 27:1925–1935. doi:[10.1029/91wr00941](https://doi.org/10.1029/91wr00941)
- Singh VP, Xu CY (1997) Evaluation and generalization of 13 mass-transfer equations for determining free water evaporation. *Hydrol Process* 11:311–323
- Skrzypek G, Mydlowski A, Dogramaci S, Hedley P, Gibson JJ, Grierson PF (2015) Estimation of evaporative loss based on the stable isotope composition of water using Hydrocalculator. *J Hydrol* 523:781–789. doi:[10.1016/j.jhydrol.2015.02.010](https://doi.org/10.1016/j.jhydrol.2015.02.010)
- Steinbruch F, Weise SM (2014) Analysis of water stable isotopes fingerprinting to inform conservation management: lake Urema Wetland System, Mozambique. *Phys Chem Earth* 72–75:13–23. doi:[10.1016/j.pce.2014.09.007](https://doi.org/10.1016/j.pce.2014.09.007)
- Sun Z, Wang H (2009) Influences and Countermeasure to ecological environment Dezhou groundwater mining creates changes and countermeasure. *Groundwater* 31(30–32):79
- Telmer K, Veizer J (2000) Isotopic constraints on the transpiration, evaporation, energy, and gross primary production budgets of a large boreal watershed: Ottawa River basin, Canada. *Glob Biogeochem Cycles* 14:149–165. doi:[10.1029/1999gb900078](https://doi.org/10.1029/1999gb900078)
- Tweed S, Leblanc M, Cartwright I, Favreau G, Leduc C (2011) Arid zone groundwater recharge and salinisation processes; an example from the Lake Eyre Basin, Australia. *J Hydrol* 408:257–275. doi:[10.1016/j.jhydrol.2011.08.008](https://doi.org/10.1016/j.jhydrol.2011.08.008)
- Van den Akker J, Simmons CT, Hutson JL (2011) Use of stable isotopes deuterium and oxygen-18 to derive evaporation from flood irrigation on the basis of pan evaporation techniques. *J Irrig Drain Eng Asce* 137:765–778. doi:[10.1061/\(asce\)ir.1943-4774.0000361](https://doi.org/10.1061/(asce)ir.1943-4774.0000361)
- Wang L et al (2012) Monitoring of selected estrogenic compounds and estrogenic activity in surface water and sediment of the Yellow River in China using combined chemical and biological tools. *Environ Pollut* 165:241–249. doi:[10.1016/j.envpol.2011.10.005](https://doi.org/10.1016/j.envpol.2011.10.005)
- Wang S, Tang C, Song X, Wang Q, Zhang Y, Yuan R (2014) The impacts of a linear wastewater reservoir on groundwater recharge and geochemical evolution in a semi-arid area of the Lake Baiyangdian watershed, North China Plain. *Sci Total Environ* 482:325–335. doi:[10.1016/j.scitotenv.2014.02.130](https://doi.org/10.1016/j.scitotenv.2014.02.130)
- Wood WW, Sanford WE (1995) Chemical and isotopic methods for quantifying ground-water recharge in a regional, semiarid environment. *Groundwater* 33:458–468. doi:[10.1111/j.1745-6584.1995.tb00302.x](https://doi.org/10.1111/j.1745-6584.1995.tb00302.x)
- Wu X, Li F, Guo J, Liu Q, Song S, Zhao G (2011) Security evaluation of nitrate and ammonium nitrogen in main river reaches of irrigation districts in downstream of Yellow River. *J Water Resour Water Eng* 22:114–117
- Xu CY, Singh VP (1998) Dependence of evaporation on meteorological variables at different time-scales and intercomparison of estimation methods. *Hydrol Process* 12:429–442. doi:[10.1002/\(SICI\)1099-1085\(19980315\)12:3<429:AID-HYP581>3.0.CO;2-A](https://doi.org/10.1002/(SICI)1099-1085(19980315)12:3<429:AID-HYP581>3.0.CO;2-A)
- Xu C, Gong L, Jiang T, Chen D, Singh VP (2006) Analysis of spatial distribution and temporal trend of reference evapotranspiration and pan evaporation in Changjiang (Yangtze River) catchment. *J Hydrol* 327:81–93. doi:[10.1016/j.jhydrol.2005.11.029](https://doi.org/10.1016/j.jhydrol.2005.11.029)
- Yakir D, Sternberg LDL (2000) The use of stable isotopes to study ecosystem gas exchange. *Oecologia* 123:297–311. doi:[10.1007/s004420051016](https://doi.org/10.1007/s004420051016)

- Yang LZ, Zhang GH, Liu ZY, Liu CH (2009) Isotope age of groundwater in Lubei Plain and evaluation of its renewable capacity. *Acta Geosci Sin* 30:235–242. doi:[10.3975/cagsb.2014.02.04](https://doi.org/10.3975/cagsb.2014.02.04)
- Zhang Y, Shen Y, Sun H, Gates JB (2011) Evapotranspiration and its partitioning in an irrigated winter wheat field: a combined isotopic and micrometeorologic approach. *J Hydrol* 408:203–211. doi:[10.1016/j.jhydrol.2011.07.036](https://doi.org/10.1016/j.jhydrol.2011.07.036)
- Zhang Y, Li F, Zhang Q, Li J, Liu Q (2014) Tracing nitrate pollution sources and transformation in surface- and ground-waters using environmental isotopes. *Sci Total Environ* 490:213–222. doi:[10.1016/j.scitotenv.2014.05.004](https://doi.org/10.1016/j.scitotenv.2014.05.004)